

NEAR POINT LIGHT SOURCES FOR SHAPE FROM SHADING*

SHENG-LIANG KAO and CHIOU-SHANN FUH

*Department of Computer Science and Information Engineering
National Taiwan University, Taipei, Taiwan*

In this paper, a linear algorithm^{3,4} is proposed to recover shape information from multiple images, each of them is taken under the environment that all of the object surfaces are illuminated by a known near point light source. In this method, an approximate range of the distance for the objects to the viewer (e.g. camera) is previously defined. Using this predefined value, the absolute depth map of the objects can be found out.

Keywords: Shape from shading, near point light sources.

1. INTRODUCTION

The image formation of a three-dimensional object mainly depends on its shape, its reflectance properties and the distribution of the light source. In addition, how the viewer (e.g. a camera) perceives this illuminated object also affects the image formation, e.g. perspective or orthographic projection, lens distortion, sensor gain, lens collection, etc. Therefore, in order to recover the original shape of the illuminated object, it is necessary to find out those parameters that affect the formation of images, such as the position of the point light source, the incident radiance and direction, the material of the object surface (e.g. Lambertian surface), parameters of the camera. After these parameters have been determined, the shape information, such as the depth map or surface gradient can then be recovered.

In fact, most of the shape recovery methods have to assume that the image formation should occur in some special conditions, for example, no specular surface, smoothness property, the number of the light source, etc.

Since the image formation is affected by the surface orientation, different parts of the surface which are oriented differently will appear with different brightness. This spatial variation of brightness can be used to estimate the orientation of surface patches. Shape from shading is one of the methods that assumes some properties of the image-formation environment and then uses different brightness distribution on the image to recover the orientations of the object surfaces.¹ Currently, the shape-from-shading problem can be solved either from a single image or from a number of images taken under different lighting conditions. The former has been developed and solved by Horn and Ikeuchi.^{1,2} He first derived a relaxation algorithm. Later, other methods, with some restrictions on the illuminated surface, were developed.⁵

*This research work was supported by National Science Council of Taiwan, ROC, under Grants NSC 85-2212-E-002-077 and NSC 86-2212-E-002-025, by Mechanical Industry Research Laboratories, Industrial Technology Research Institute under Grant MIRL 863K67BN2, by EeRise Corporation, ACME Systems, Mosel Vitelic and Foxconn Inc.

Another kind of algorithms for the shape-from-shading problem is the photometric stereo method. This method requires multiple images of the same view which are taken under different lighting conditions. The photometric stereo method which Woodham⁷ has worked on is simple to implement, but requires control of the lighting.

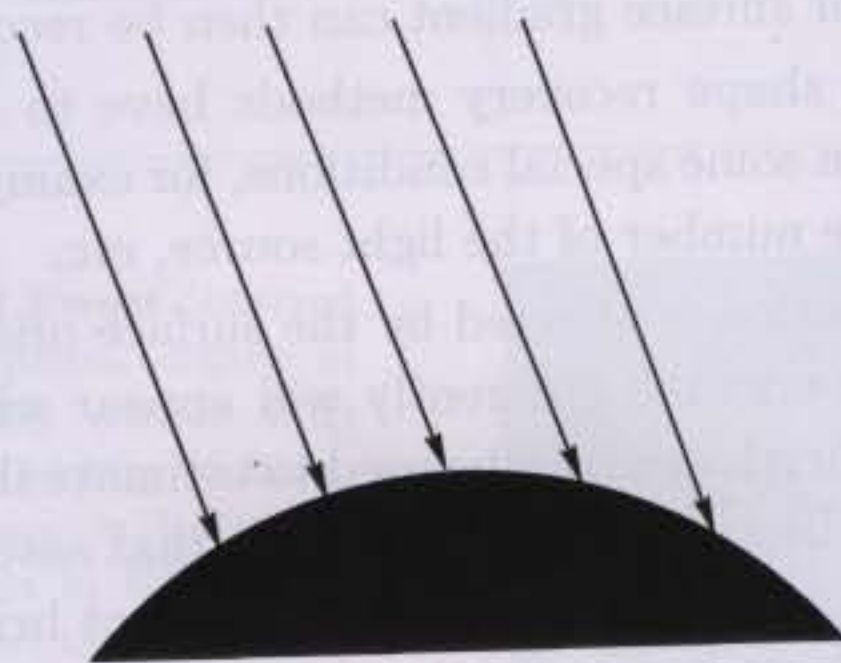
1.1. Distant Point Light Source

Since the difference in the lighting condition will affect the formation of images, the position of the light source should be considered. When there is a point light source distant from the illuminated surface (for example, the sun can be a point light source when it is viewed on the earth), the incident direction for any illuminated point on the surface will be the same as shown in Fig. 1. Therefore, the incident angle will be determined by the surface normal vector. In the previous work,¹ an equation for the variety of irradiance on the illuminated object has been derived and the irradiance equation can be combined with the reflectance map. The reflectance map includes the relationship between surface orientation and brightness. Therefore, if other image-formation parameters about the camera (e.g. the lens gain) are constants, the image intensity equation can be constructed by the irradiance equation.⁶ Given an image $I(x, y)$ and a reflectance map $R(p, q)$, the image intensity equation can be represented as

$$I(x, y) = \rho s_0 R(p, q)$$

where ρ is the reflectance factor (i.e. albedo), s_0 is the incident radiance.

from a distant point light source



the illuminated object

Fig. 1. For a distant point light source, the incident direction is always the same on the illuminated surface.

If the surface has the Lambertian property, which means that the surface appears to be of equal radiance from all viewing directions, and is illuminated by an ideal point light source, then the reflectance map can be expressed as

$$R(p, q) = \cos \theta_i = \frac{\mathbf{s} \cdot \mathbf{n}}{\|\mathbf{s}\| \|\mathbf{n}\|} \quad (1)$$

where θ_i is the angle between the surface normal vector \mathbf{n} and the incident light source direction \mathbf{s} . After rewriting the image intensity equation and substituting (S_x, S_y, S_z) and $(p, q, -1)$ for the incident direction of the distant point light source and the surface gradient at the illuminated point, respectively, the image intensity can be expressed as

$$I(x, y) = \rho s_0 \frac{S_x p + S_y q - S_z}{(p^2 + q^2 + 1)^{\frac{1}{2}}}. \quad (2)$$

If the illuminated surface has Lambertian property $\rho \cdot s_0$ should be a constant. Under the assumption that the single point light source is distant from the object and the direction \mathbf{s} is known, the above equation can be used to derive the orientation of the object surface from a single or multiple images.

There are two major methods for this, one is the partial differential equation method, the other is the photometric stereo method. Horn¹ was the first one undertaking the former study and subsequent improvements. Woodham⁷ used the photometric method to determine the surface orientation. In the next section, we will briefly introduce the photometric method.

1.2. Near Point Light Source

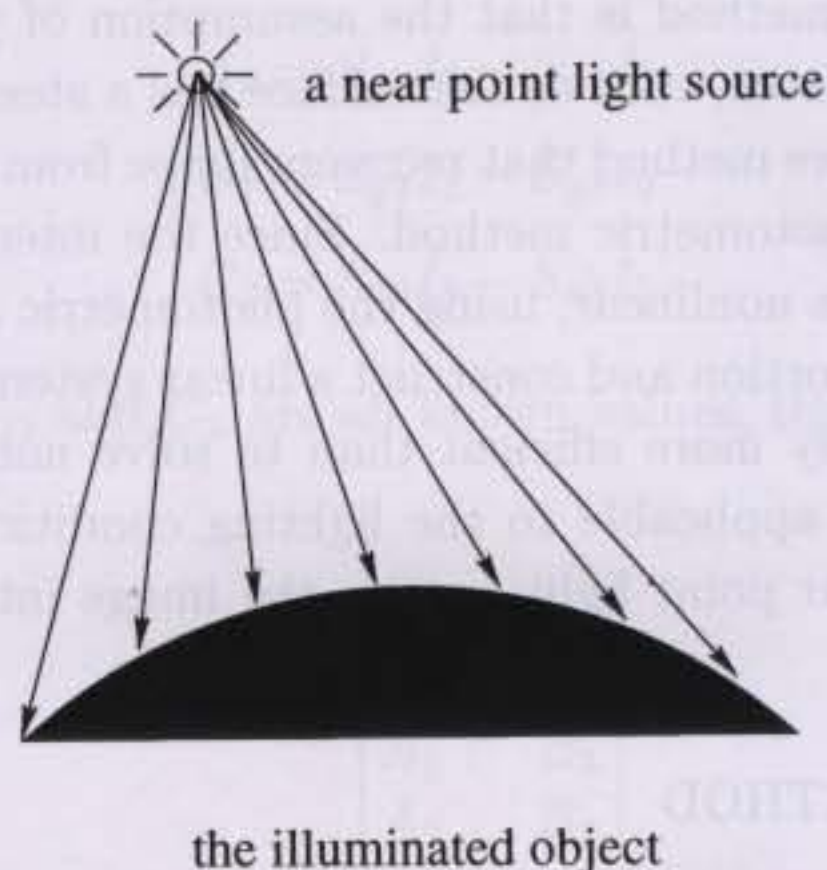


Fig. 2. For a near point light source, the incident direction depends on the coordinates of the light source and the illuminated point.

Equation (1) is valid under the assumption that the point light source is distant from the illuminated surface, that is, all incident light directions are the same, as shown in Fig. 1. However, when the point light source is near the illuminated surface, as shown in Fig. 2, the incident direction as well as the incident radiance is not a constant for this surface anymore. Furthermore, the distance between the surface point and the point light source must be taken into consideration.

After taking these changes into consideration, some modifications⁶ are made on the image intensity. The new intensity equation can be expressed as

$$I(x, y) = \rho s_0 \frac{(P_S - P_O) \cdot \mathbf{n}}{\|P_S - P_O\|^3 \|\mathbf{n}\|} \quad (3)$$

where ρ , s_0 , and \mathbf{n} have been defined in Eq. (1), P_S is the Cartesian coordinate of the near point light source, and P_O is the Cartesian coordinate of the illuminated point.

If the illuminated point is orthographically projected on the image, we can rewrite Eq. (3) in detail as the following⁶:

$$I(x, y) = k \cdot \frac{(S_x - x)p + (S_y - y)q - (S_z - z)}{[(S_x - x)^2 + (S_y - y)^2 + (S_z - z)^2]^{\frac{3}{2}} \cdot (p^2 + q^2 + 1)^{\frac{1}{2}}} \quad (4)$$

where k is the product of ρ , s_0 ; (x, y, z) is the Cartesian coordinate of the illuminated surface; (S_x, S_y, S_z) is the Cartesian coordinate of the point light source; (p, q) is the gradient of the surface at the illuminated point.

Rashid and Burger⁶ have used a differential method to determine the gradient. They assumed that the point light source was near the camera (the projection center) and small surface patches on the objects were assumed nearly planar. Using a small planar surface patch, this method could determine the surface normal vector using the first-order and second-order differentials of the image intensities. The shortcoming of the method is that the assumption of planar surface patch is inapplicable to some surfaces, such as the surface has a steep orientation.

In contrast to the above method that recovers shape from a single image, another kind of method is the photometric method. Since the intensity equation with the unknown normal vector is nonlinear, using the photometric approach, it may easily eliminate the nonlinear portion and construct a linear system of equations. To solve linear equations is usually more efficient than to solve nonlinear ones. However, such elimination is only applicable to the lighting condition as the distant point light source. For the near point light source, the image intensity equation should be further considered.

2. PHOTOMETRIC METHOD

As described above, the image intensity equation, either for the distant point light source or for the near point light source, has some variables which make the equation a nonlinear one.⁷ If only one image exists, we can either directly solve this equation using complex mathematics or consider the whole surface patch and find out an optimal solution.^{1,6} However, if there are two or more images of the same scene but with different illuminating light sources, we can reduce the problem to solve a system of equations.⁷ For example, if some illuminated point at which the surface gradient is (p, q) , is orthographically projected from the Cartesian coordinate (x, y, z) onto the coordinate (x, y) of the image plane. Suppose three different distant point light sources individually illuminate this point in three different images. The incident

directions of these three point light sources are assumed to be the unit vectors (S_{x3}, S_{y3}, S_{z3}) , (S_{x2}, S_{y2}, S_{z2}) , and (S_{x1}, S_{y1}, S_{z1}) . Using Eq. (2), these three image intensities for this illuminated point can be written as

$$I_1(x, y) = \rho s_0 \frac{S_{x1}p + S_{y1}q - S_{z1}}{(p^2 + q^2 + 1)^{\frac{1}{2}}}, \quad (5)$$

$$I_2(x, y) = \rho s_0 \frac{S_{x2}p + S_{y2}q - S_{z2}}{(p^2 + q^2 + 1)^{\frac{1}{2}}}, \quad (6)$$

$$I_3(x, y) = \rho s_0 \frac{S_{x3}p + S_{y3}q - S_{z3}}{(p^2 + q^2 + 1)^{\frac{1}{2}}}. \quad (7)$$

Divide Eqs. (5) and (6) by Eq. (7). On simplifying the coefficients and rearranging the equations, a system of linear equations with two unknown values can be extracted.

$$\begin{cases} A_1p + B_1q = C_1 \\ A_2p + B_2q = C_2 \end{cases} \quad (8)$$

where

$$A_1 = S_{x1}I_3 - S_{x3}I_1$$

$$B_1 = S_{y1}I_3 - S_{y3}I_1$$

$$C_1 = S_{z1}I_3 - S_{z3}I_1$$

$$A_2 = S_{x2}I_3 - S_{x3}I_2$$

$$B_2 = S_{y2}I_3 - S_{y3}I_2$$

$$C_2 = S_{z2}I_3 - S_{z3}I_2.$$

Since A_1, B_1, C_1, A_2, B_2 , and C_2 are all known values, the surface gradient can be directly solved.

$$p = \frac{\begin{vmatrix} C_1 & B_1 \\ C_2 & B_2 \end{vmatrix}}{\begin{vmatrix} A_1 & B_1 \\ A_2 & B_2 \end{vmatrix}} \quad (9)$$

$$q = \frac{\begin{vmatrix} A_1 & C_1 \\ A_2 & C_2 \end{vmatrix}}{\begin{vmatrix} A_1 & B_1 \\ A_2 & B_2 \end{vmatrix}} \quad (10)$$

Since this method requires the known positions of the point light sources, the difficulty arises in controlling the light source.

Unlike illuminating with distant point light sources, the system of intensity equations for near point light sources is difficult to reduce to linear equations as above. In the previous work,^{3,4} a method using the photometric concept to solve the shape

from shading with near point light sources has been proposed. Using this algorithm, we have to take four images with different point light sources. Furthermore, these point light sources must be very close to others such that the distance component in the intensity equation can be ignored. Finally, use the infinitesimal differences among these images to solve the shape information. However, this method can be very unstable if these point light sources are not placed properly.

3. THE APPROXIMATE SOLUTION CURVE TRACING (ASCT) METHOD

For the image of an illuminated surface using a near point light source, the intensity equation can be expressed as Eq. (4). If the position of the point light source (S_x, S_y, S_z) is known and the image is taken by orthographic projection, there will exist four unknown values in the intensity equation. These unknown values are the reflectance factor k , the depth value z , and the gradient (p, q) . (Note that the image intensity is known.) If the photometric method is used to solve these unknown values, at least three or four images are needed. However, there is a difference between the application of the photometric method to the distant and near point light sources. In the case of distant point light sources, only three images with different illuminated sources are sufficient for solving the unknown values. The reason is that there are only three unknown values (including the reflectance factor k) in the intensity equation for a distant point light source (that is, Eq. (2)) and a system of linear equations can be generated by the division as described in Sec. 2. Since the intensity equation for a near point light source (that is, Eq. (4)) is very different from Eq. (2), the procedure which is used to solve unknown values in Eq. (2) is inapplicable to Eq. (4). The difficulty is that the expression $[(S_x - x)^2 + (S_y - y)^2 + (S_z - z)^2]^{\frac{3}{2}}$ in Eq. (4), is a nonlinear function of the depth value z and this function varies according to the position of the point light source (S_x, S_y, S_z). If the same procedure is applied to Eq. (4), a system of nonlinear equations will be derived. It is hard to solve such equations.

Instead of deriving solutions like Eqs. (9) and Eq. (10) from multiple input images, the algorithm proposed in this paper will use a method like the photometric stereo to search solutions in a predefined range. Before introducing the method, we first define some terminologies.

3.1. The Correct Solution Space (CSS)

For every illuminated surface, there exists a depth map based on the lens as described previously. If the thickness of the illuminated object is finite, we can assume that there exists a range to include all of the depth values of the points on the surface. We call the range *correct solution space* (CSS). However, how can we find out the range?

First, as in Fig. 3, since these point light sources are near the illuminated surface, the depth values of these point light sources are the most suitable value to estimate the CSS. It is easy to hypothesize a depth value that is "deeper" than all depth values on the illuminated surface. This depth value is the lower bound of the CSS

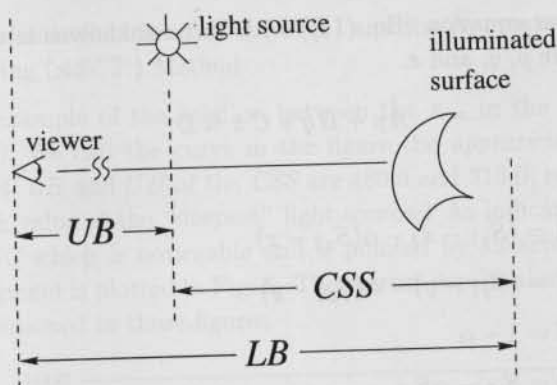


Fig. 3. The *CSS* represents the *correct solution space* in which all depth values on the illuminated object have been included. *LB* is the lower bound of the *CSS*. All depth values on the illuminated object will not be "deeper" than it. *UB* is the upper bound of the *CSS*. All depth values on the illuminated object are always "deeper" than it.

and can be represented as *LB*. Likewise, since the illumination model currently assumes that the depth value of the light source is always less than the depth values of the illuminated points, the depth value of the light source can be used as the upper bound of the *CSS*. We call this upper bound *UB*. Therefore, the *CSS* will be bound with the two values, *LB* and *UB*.

3.2. The Approximate Solution Difference (*ASD*)

According to the foregoing description, the system of equations which is derived from Eq. (4) using the photometric method will be nonlinear equations. The major problem is the function of z , $[(S_x - x)^2 + (S_y - y)^2 + (S_z - z)^2]^{\frac{3}{2}}$ in Eq. (4). Therefore, we introduce an approximate value for this function here to simplify the problem. As we have defined in Sec. 3.1, there exists a range (named the *CSS*) in which all possible depth values are included. If a value in the *CSS* is substituted for the unknown value, z , in the expression $[(S_x - x)^2 + (S_y - y)^2 + (S_z - z)^2]^{\frac{3}{2}}$, an approximate value for this nonlinear function is obtained. This value is the cube of the approximate distance between the light source and the illuminated point.

Now suppose we have two images I_1, I_2 , the corresponding point light sources are (S_{x1}, S_{y1}, S_{z1}) and (S_{x2}, S_{y2}, S_{z2}) , the illuminated point is (x, y, z) , and the normal vector is $(p, q, -1)$. The two image intensities in I_1 and I_2 can be expressed as (note that the projection of the image is orthographic)

$$I_1(x, y) = k \cdot \frac{(S_{x1} - x)p + (S_{y1} - y)q - (S_{z1} - z)}{[(S_{x1} - x)^2 + (S_{y1} - y)^2 + (S_{z1} - z)^2]^{\frac{3}{2}}(p^2 + q^2 + 1)^{\frac{1}{2}}}, \quad (11)$$

$$I_2(x, y) = k \cdot \frac{(S_{x2} - x)p + (S_{y2} - y)q - (S_{z2} - z)}{[(S_{x2} - x)^2 + (S_{y2} - y)^2 + (S_{z2} - z)^2]^{\frac{3}{2}}(p^2 + q^2 + 1)^{\frac{1}{2}}}. \quad (12)$$

Substitute a value in the *CSS*, called z_{CSS} , for the unknown variable z in the denominator of both equations and divide Eq. (11) by Eq. (12). After simplifying the

coefficients, a linear equation (Eq. (13)) with three unknowns is obtained. These unknown values are p , q , and z .

$$Ap + Bq + Cz = D \quad (13)$$

where

$$A = (S_{x1} - x) - \alpha(S_{x2} - x)$$

$$B = (S_{y1} - y) - \alpha(S_{y2} - y)$$

$$C = 1 - \alpha$$

$$D = S_{z1} - \alpha S_{z2}$$

$$\alpha = \frac{I_1 \cdot [(S_{x1} - x)^2 + (S_{y1} - y)^2 + (S_{z1} - z_{css})^2]^{\frac{3}{2}}}{I_2 \cdot [(S_{x2} - x)^2 + (S_{y2} - y)^2 + (S_{z2} - z_{css})^2]^{\frac{3}{2}}}$$

z_{css} = a value in the CSS.

In order to solve the unknown values, another two equations like Eq. (13) are needed. In other words, at least four images with different point light sources are needed to construct three linear equations with three unknown values as Eq. (13). For example, we name the four images as I_1 , I_2 , I_3 , and I_4 and pair these images (e.g. I_1/I_2 , I_2/I_3 , and I_3/I_4). In addition, all of these equations use the same z_{css} . Suppose these generated linear equations are

$$\begin{cases} A_1p + B_1q + C_1z = D_1 \\ A_2p + B_2q + C_2z = D_2 \\ A_3p + B_3q + C_3z = D_3 \end{cases} \quad (14)$$

where A_i , B_i , C_i , and D_i ($i = \{1, 2, 3\}$) are similarly derived from the i th pair of images by the procedure which derives Eq. (13). Thus we can obtain a solution for the z value in the system of equations.

$$z_{app} = \frac{\begin{vmatrix} A_1 & B_1 & D_1 \\ A_2 & B_2 & D_2 \\ A_3 & B_3 & D_3 \end{vmatrix}}{\begin{vmatrix} A_1 & B_1 & C_1 \\ A_2 & B_2 & C_2 \\ A_3 & B_3 & C_3 \end{vmatrix}} \quad (15)$$

We call the solution, z_{app} , the *approximate solution* (AS) and the difference function

$$\Delta Z(z_{css}) = z_{app} - z_{css} \quad (16)$$

is called the *approximate solution difference* (ASD). This function is a function of z_{css} and the domain of z_{css} is in CSS. In Sec. 3.3, we will show how the ASD changes as z_{css} varies in the domain CSS and what happens if z_{css} is the correct depth value of the illuminated point.

3.3. The Approximate Solution Curve (ASC) and the Approximate Solution Curve Tracing (ASCT) Method

Figure 4 is an example of the relation between the z_{CSS} in the CSS and the corresponding ASD. We call the curve in the figure the *approximate solution curve* (ASC). In Fig. 4, LB and UB of the CSS are 480.0 and 315.0, respectively. (315.0 is also the depth value of the "deepest" light source.) As indicated, there is a segment of the ASC which is noticeable and is pointed by an arrow in Fig. 4. The details of the segment is plotted in Fig. 5. The correct depth value of the illuminated point is also mentioned in these figures.

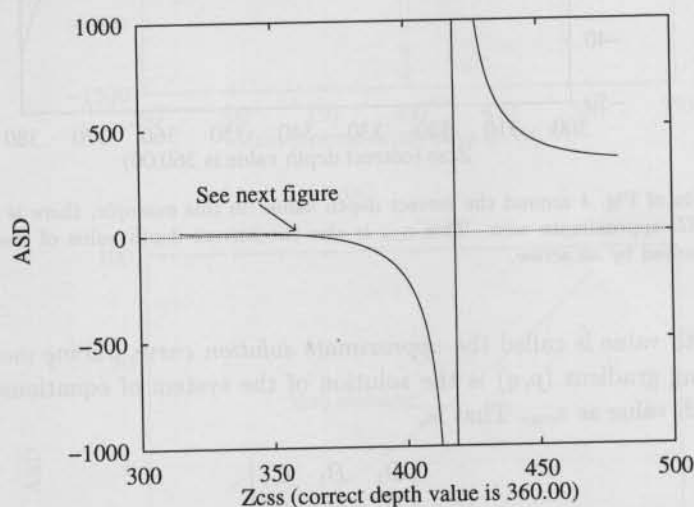


Fig. 4. An example of the relation between the z_{CSS} in the CSS and the corresponding ASD. There is a singular value at $z_{CSS} = 418.46$ in this figure. The position of the singular value is also "deeper" than the correct depth value of the illuminated point. Therefore, this singular value may not appear in the ASC. It depends on the choice of the LB of the CSS. Other details are plotted in Fig. 5.

In this example of the ASC, there exists a singular value at $z_{CSS} = 418.46$. Figure 4 shows the detail around the singular value. On the left-hand side of the singular value, the ASD is close to positive infinity; on the right-hand side of the singular value, the ASD is close to negative infinity. The position of the singular value is also "deeper" (that is, more distant from the lens) than the correct depth value of the illuminated point. If the LB of the CSS is chosen such that the range of CSS is smaller (for example, $LB = 410.0$ and UB not changed), this singular value will not appear in the ASC. Therefore, the existence of the singular value depends on the choice of the LB of the CSS.

Figure 5 shows the zoom-in of the ASC around the correct depth value of the illuminated point. Obviously, if z_{CSS} is equal to the correct depth value of the illuminated point, the ASD is zero. Therefore, if the range of the CSS is properly chosen, the correct depth value of the illuminated point can be found by tracing the ASC in the range of CSS until a z_{CSS} makes the ASD zero. This way of finding

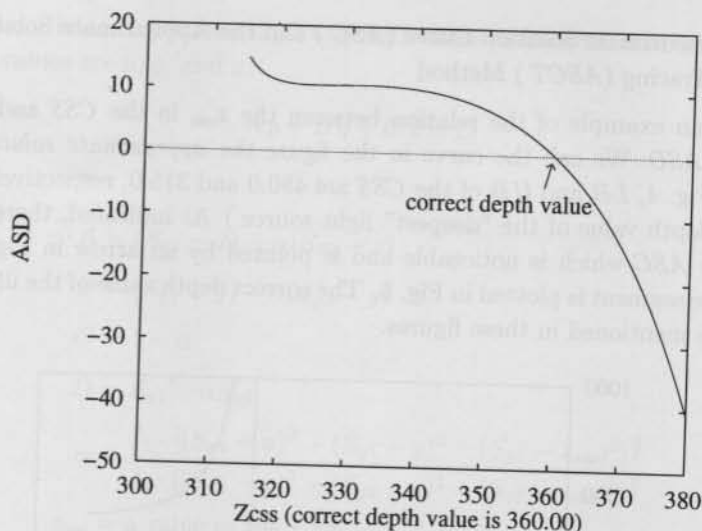


Fig. 5. Zoom-in of Fig. 4 around the correct depth value: in this example, there is a z_{css} which makes the ASD approximate zero. This z_{css} is also the correct depth value of the illuminated point. It is pointed by an arrow.

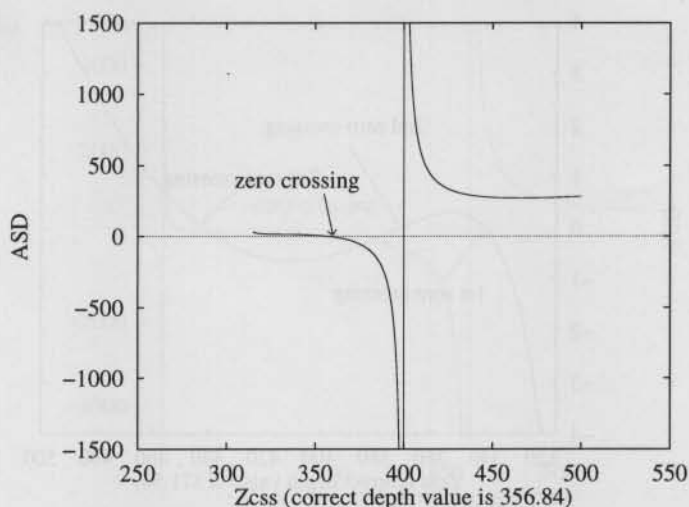
out the depth value is called the *approximate solution curve tracing* method. The corresponding gradient (p, q) is the solution of the system of equations using the correct depth value as z_{css} . That is,

$$p = \frac{\begin{vmatrix} D_1 & B_1 & C_1 \\ D_2 & B_2 & C_2 \\ D_3 & B_3 & C_3 \end{vmatrix}}{\begin{vmatrix} A_1 & B_1 & C_1 \\ A_2 & B_2 & C_2 \\ A_3 & B_3 & C_3 \end{vmatrix}} \quad (17)$$

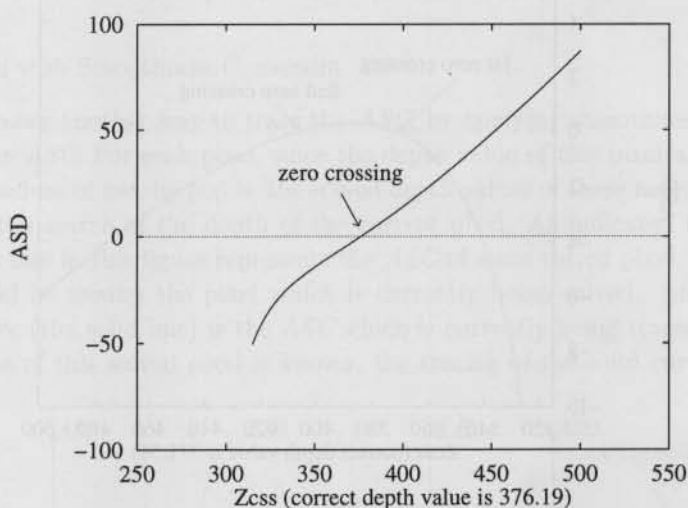
$$q = \frac{\begin{vmatrix} A_1 & D_1 & C_1 \\ A_2 & D_2 & C_2 \\ A_3 & D_3 & C_3 \end{vmatrix}}{\begin{vmatrix} A_1 & B_1 & C_1 \\ A_2 & B_2 & C_2 \\ A_3 & B_3 & C_3 \end{vmatrix}} \quad (18)$$

where A_i , B_i , C_i , and D_i ($i = \{1, 2, 3\}$) have been defined except that z_{css} is the known correct depth value.

The ASC shown in this section is a typical of the possible ASCs. Most ASCs have such a profile. There are other ASCs with different profiles. Figures 6–8 are examples for other profiles.



(a)



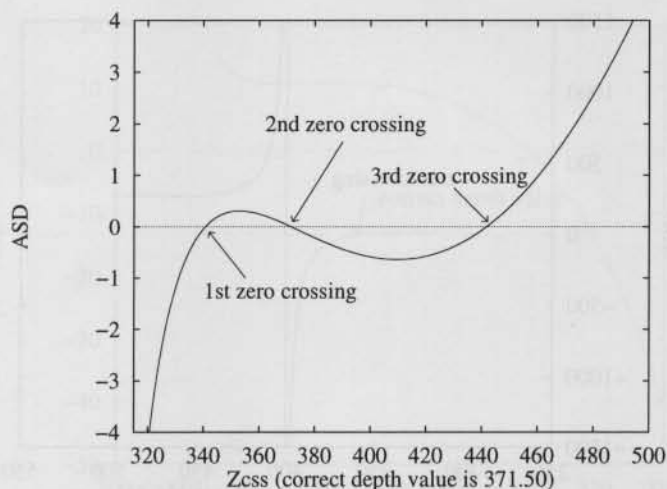
(b)

Fig. 6. (a) *Infinity* profile: there exists a singular value and a zero crossing in *CSS* and this singular value can be on either side of the zero crossing. (b) *Slope* profile: the *ASC* is monotonically increasing or decreasing in the *CSS*.

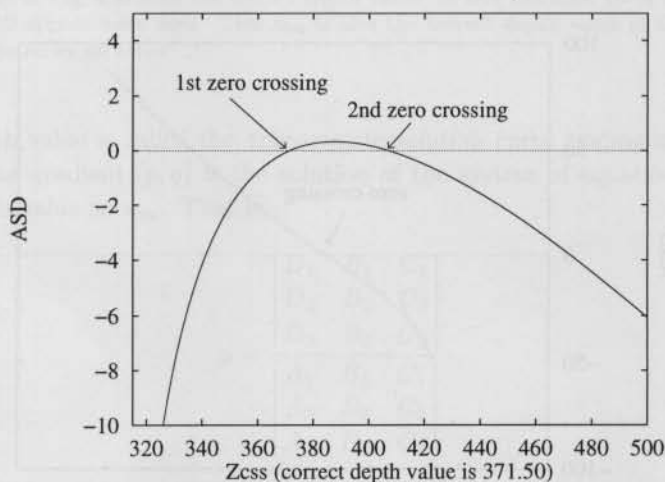
4. IMPLEMENTATION

4.1. Exhaustive Search

In order to find out all $z_{css}(s)$ at which zero crossings appear, examining the whole *CSS* (i.e. the exhaustive search method) is the simplest method. As described in Sec. 3, multiple zero crossings are possible. However, since *ASCs* with one zero crossing occurs more frequently than others, a simple method to select the correct



(a)



(b)

Fig. 7. (a) *Double-curve* profile: a local minimum, a local maximum, and three (or one, depending on the local minimum and maximum) zero crossings appear in this profile. (b) *Cap* profile: a local maximum and two (or one, depending on the local minimum and maximum) zero crossings appear in this profile.

depth value from multiple zero crossings is required. Usually, the surface of the illuminated object can be assumed to be continuous or smooth. Therefore, if one of the neighbor pixels is solvable (solved either by smoothness constraint or by only one zero crossing), by smoothness constraint, the correct depth value should be the zero crossing that is closest to the depth of the neighbor.

Although exhaustive search is one of the algorithms that trace the *ASC*, much time is spent on tracing the *ASC* for each pixel. All pixels which are solvable take the same time to trace the *ASCs* in the same *CSS*.

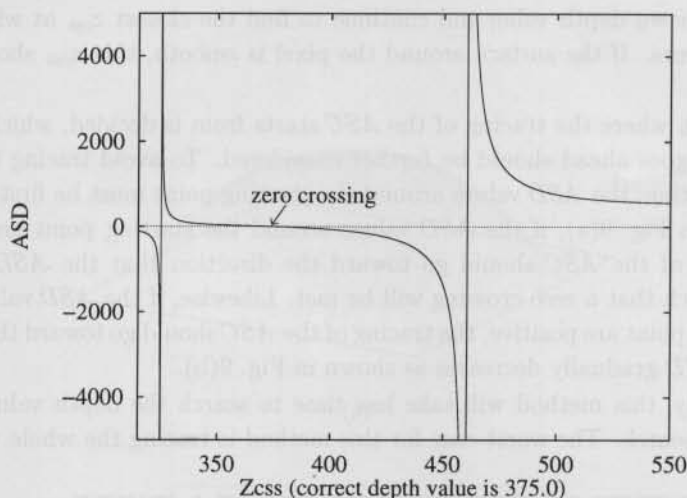


Fig. 8. Double-infinity profile: these kinds of curves have two singular values in the corresponding CSS.

4.2. Search with Smoothness Constraint

Figure 9 shows another way to trace the *ASC*, by applying smoothness constraint to trace the *ASC*. For each pixel, since the depth value of this pixel approximates the depth values of nearby pixels, the solved depth values of these nearby pixels are useful for the search of the depth of the current pixel. As indicated in Fig. 9(a), the broken line in this figure represents the *ASC* of some solved pixel. This solved pixel should be nearby the pixel which is currently being solved. Another curve in the figure (the solid line) is the *ASC* which is currently being traced. Since the depth value of this solved pixel is known, the tracing of the solid curve can start

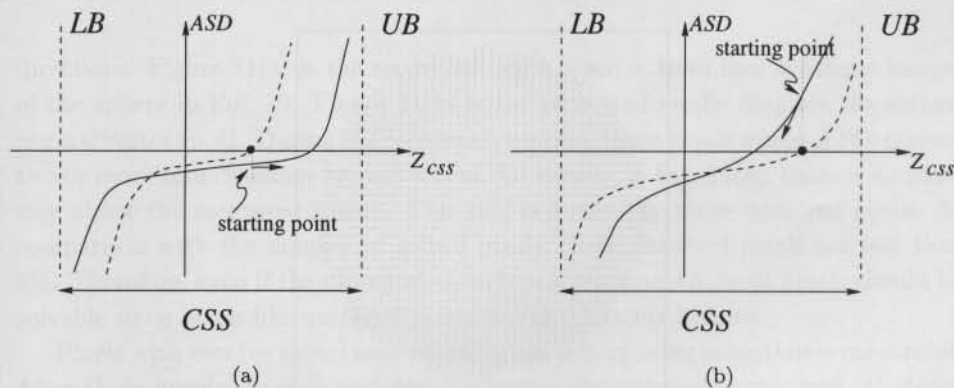


Fig. 9. The broken lines in these figures represent the *ASC* of some pixel which has been solved and this pixel should be adjacent to the currently solving pixel whose *ASC* is plotted with solid lines. In both figures, the solid curves are traced from the starting point and going toward the indicated directions.

from this known depth value and continue to find the closest z_{css} at which a zero crossing occurs. If the surface around the pixel is smooth, this z_{css} should be the depth value.

Although where the tracing of the *ASC* starts from is decided, which direction the tracing goes ahead should be further considered. To avoid tracing toward the wrong direction, the *ASD* values around the starting point must be first examined. As shown in Fig. 9(a), if the *ASD* values around the starting point are negative, the tracing of the *ASC* should go toward the direction that the *ASD* gradually increases such that a zero crossing will be met. Likewise, if the *ASD* values around the starting point are positive, the tracing of the *ASC* should go toward the direction that the *ASD* gradually decreases as shown in Fig. 9(b).

Evidently, this method will take less time to search the depth value than the exhaustive search. The worst case for this method is tracing the whole *CSS*.

5. EXPERIMENTS ON SYNTHETIC IMAGES OF A SPHERE

Figure 10(a) is a synthetic sphere and Fig. 10(b) is the corresponding needle diagram.¹ We use a sphere because the normal vectors of a sphere cover all

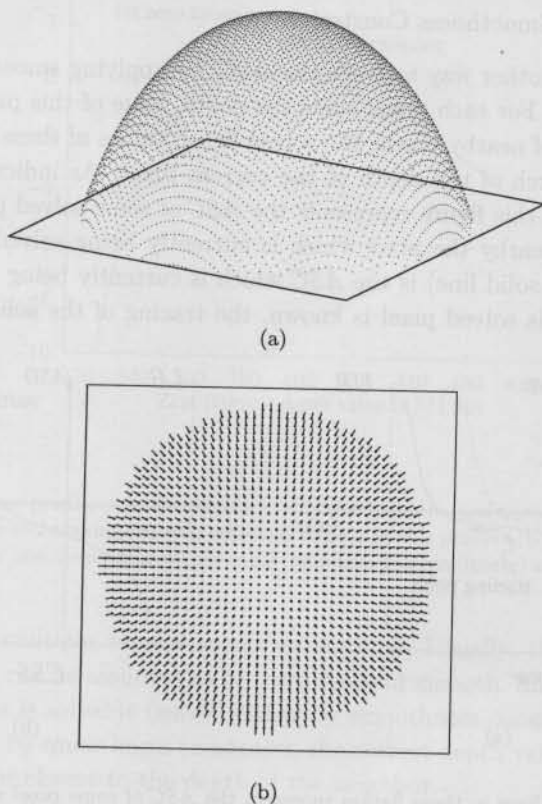
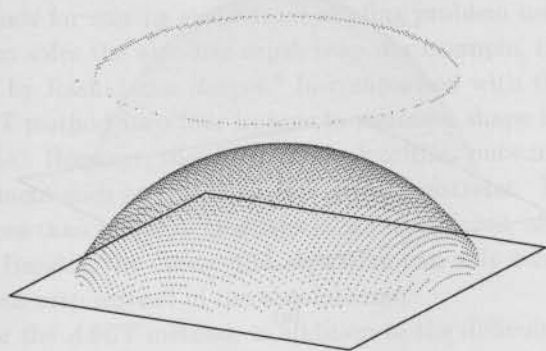
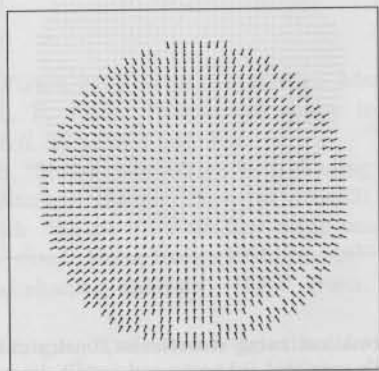


Fig. 10. Original shape of a synthetic sphere. (a) Depth map, z , and (b) needle diagram for surface normal vector (p, q) .



(a)



(b)

Fig. 11. Recovered shape information: without solving those pixels that have two or more zero crossings in their ASCs. (a) Recovered depth map and (b) recovered needle diagram.

directions. Figure 11(a) is the recovered depth map, z , from four synthetic images of the sphere in Fig. 10. Figure 11(b) is the recovered needle diagram for surface normal vector (p, q) . During the recovering process, those pixels whose ASCs possess two or more zero crossings are not solved. Obviously, in Fig. 11(a), there is a sparse ring above the recovered sphere. This ring is formed by those unsolved pixels. In comparison with the number of solved pixels, these unsolved pixels are less than 5%. Therefore, even if the illuminated surface is not smooth, most pixels should be solvable since pixels like unsolved pixels in Fig. 11 rarely happen.

Pixels with two (or more) zero crossings are solved using smoothness constraint. After these unsolved pixels with two (or more) zero crossings are solved, all depth values are plotted again in Fig. 12. These experiments on synthetic images has error of 0.01% on the depth map. Our algorithm takes about 90 seconds when the image size is 64×64 and runs on SUN Sparcstation 2.

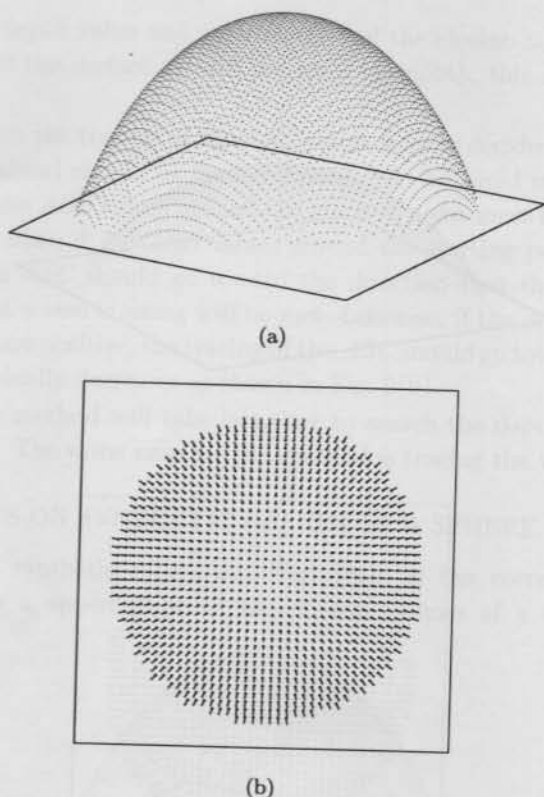


Fig. 12. Recovered shape information: using smoothness constraint to solve those unsolved pixels in Fig. 11. (a) Recovered depth map and (b) recovered needle diagram.

6. CONCLUSION

In this paper, we propose a method to find out absolute depth values of three-dimensional objects from a predefined range and the surface orientation can be also calculated.

In Sec. 1, when comparing intensity equations, it is obvious that if objects are illuminated by distant point light source, algorithms for solving the shape-from-shading problems can solve surface orientation and generate relative depth map from surface orientation. If objects are illuminated by near point light sources, both surface orientation and absolute depth map can be estimated. However, the former problem (distant light source) can be easily solved by photometric method and the later (near light source) should take more considerations for the intensity equation before applying the photometric method. Another difficulty when using photometric methods is the calibration of the accurate position or direction of the light source. Since errors in position of any one point light source can significantly affect the solution of the whole intensity equations, all point light sources should be carefully calibrated.

Not all methods for solving shape-from-shading problem using near point light source are able to solve the absolute depth map, for example, the differential algorithm presented by Rashid and Burger.⁶ In comparison with the differential algorithm, the *ASCT* method uses four images to estimate shape information instead of a single image. However, the differential algorithm puts more restrictions on shading environment such as planar surface patch constraint. The *ASCT* method, if the case of more than one zero crossings is not considered, almost does not need any restriction. Besides, the differential algorithm can only solve surface gradients and relative depth map instead of the absolute one.

Currently, for the *ASCT* method, in addition to the difficulty in calibrating the light source position, noises such as quantization error also significantly affect the accuracy of the depth map. Further improvements on this method are required to overcome both problems.

REFERENCES

1. B. K. P. Horn, *Robot Vision*, MIT Press, Cambridge, Massachusetts, 1986.
2. K. Ikeuchi and B. K. P. Horn, "Numerical shape from shading and occluding boundaries", *Artif. Intell.* **17** (1981) 141-184.
3. S. L. Kao and C. S. Fuh, "Shape information from shading using photometric method", *IPPR Conf. CVGIP*, Nantou, Taiwan, 1994, pp. 326-331.
4. S. L. Kao and C. S. Fuh, "Shape from shading using near point light sources", *Proc. Int. Computer Science Conf.*, Hong Kong, 1995, pp. 487-488.
5. A. P. Pentland, "Local shading analysis", *IEEE Trans. Patt. Anal. Mach. Intell.* **6** (1984) 170-187.
6. H. U. Rashid and P. Burger, "Differential algorithm for the determination of shape from shading using a point light source", *Imag. Vision Comput.* **10** (1992) 119-127.
7. R. J. Woodham, "Photometric method for determining surface orientation from multiple images", *Opt. Engin.* **19** (1980) 139-144.



Sheng-Liang Kao received the B.S. degree in computer science and information engineering from National Chiao Tung University, Hsinchu, Taiwan, in 1993, and the M.S. degree in computer science and information engineering

from National Taiwan University, Taiwan, in 1995.

He currently works for the software department in Gigabyte Technology.



Chiou-Shann Fuh received the B.S. degree in computer science and information engineering from National Taiwan University, Taipei, Taiwan, in 1983, the M.S. degree in computer science from the Pennsylvania State University,

University Park, PA, in 1987, and the Ph.D. degree in computer science from Harvard University, Cambridge, MA, in 1992. He was with AT&T Bell Laboratories and engaged in performance monitoring of switching networks from 1992 to 1993. Since 1993, he has been an associate professor in the Computer Science and Information Engineering Department at National Taiwan University, Taipei, Taiwan.

His current research interests include digital image processing, computer vision, pattern recognition and mathematical morphology.

ISSN: 0218-0014

INTERNATIONAL JOURNAL OF PATTERN RECOGNITION AND ARTIFICIAL INTELLIGENCE

Volume 12 • Number 7 • November 1998



World Scientific